ACS OMEGA

Article

Cite This: ACS Omega 2019, 4, 12342−12356

http://pubs.acs.org/journal/acsodf

Design of L-Lysine-Based Organogelators and Their Applications in Drug Release Processes

Seref Kaplan, Mehmet Colak, Halil Hosgoren, and Necmettin Pirinccioglu*

Department of Chemistry, Faculty of Science, Dicle University, 21280 Diyarbakir, Turkey

Supporting Information

ABSTRACT: This work reports on the synthesis of three new L-lysine-based organogelators bis(N^2-alkanoyl-N^6-L-lysyl ethylester)oxalylamides, where alkanoyls are lauroyl, myristoyl, and palmitoyl. The gels of these gelators were prepared with high yields in eco-friendly solvents commonly used in cosmetics such as ethyl and isopropyl esters of lauric and myristic acids, liquid paraffin, 1-decanol, and 1,2-propanediol. Fourier transform infrared measurements revealed the involvement of intermolecular hydrogen bonds in the gelation. Scanning electron microscopy images of xerogels indicated different morphologic patterns with regard to the alkanoyl chain length and the solvent employed in their preparation. The gel formation was supported by rheological measurements. Three gels prepared in liquid paraffin were loaded with naproxen (Npx) with a quite high loading capacity (up to 166.6% as percentage of gelator) without gel disruption. The release of Npx from the gel matrix into the buffered solution at physiologic pH was evaluated using UV−vis spectroscopy. The results revealed that the release rate of Npx from the organogels significantly retarded with increasing organogelator concentration, whereas it enhanced with increasing Npx concentration. The rate was also found to be pH-dependent; the lower the pH, the lower the rate. Furthermore, molecular dynamic calculations performed on the octamer of myristoyl-bearing gelator (**N^2M/N^6Lys**) in 1,2-propanediol provided useful information regarding the structural properties of the gels, which may be of interest to interpret the structure of the gel matrix. Altogether, this work provided valuable outcomes, which may be relevant to the pharmaceutical industry. It may be suggested that L-lysine-based gels have potentials in the delivery of nonsteroidal anti-inflammatory drug molecules. Besides, the release of the drug can be fine-tuned by the correct choice of gelator−solvent combination.

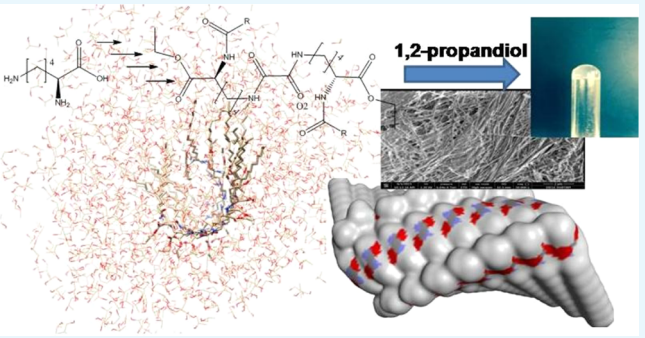

1. INTRODUCTION

The hunt for rational design of small molecules with the ability to self-assemle in a predictable way for a specific purpose has become a long journey of scientists, which is inspired by highly selective and enormous catalytic functions of macromolecules in living cells. One of the examples of these is the design of molecules with gelation properties, which have many applications,[1,2] including biomedicine, especially for tissue engineering and drug delivery.[3−13] Gels have important soft material properties, formed by self-aggregation from small low-molecular-weight compounds via noncovalent interactions, leading to immobilization of solvents.[14] If the solvent is water, the gels are called hydrogels, otherwise they are called organogels. They are largely classified as low-molecular-weight gelators (LMWGs), most of which bear short peptides or peptidomimetics.[15] Hence, the design of biocompatible LMWGs for the drug delivery forms a good stand in the field.[16] They may be derived from naturally occurring precursors such as amino acids,[17−31] carbohydrates,[32−34] and lipids.[35] Amino acids offer a good standpoint for preparing synthetic organogelators, as alternatives to the naturally occurring ones like lecithin, which are expensive and lack large-scale production. Their synthetic procedures are relatively easy and well established. Furthermore, their natural abundance makes amino acids as the main starting materials in the development of gelators.

The synthesis of the L-lysine-based gemini organogelators was originally reported by Hanabusa et al.[36] involving an oxalayl bridge joining two L-lysine units via N^2-amine sites. However, in the current study, two lysines were linked by an oxalayl bridge via N^6-amine heads. This provides an advantage since the synthesis involves a straightforward step and hence does not require any protection. The remaining free N^2-amines were then converted into amides with acid chlorides derived from naturally occurring carboxylic acids. Thus, as a result, three new L-lysine-based biocompatible gelators, bearing alkanoyl groups, bis(N^2-lauroyl-N^6-L-lysyl ethylester)-oxalylamides (**N^2L/N^6Lys**), bis(N^2-myristoyl-N^6-L-lysyl ethylester)oxalylamides (**N^2M/N^6Lys**), and bis(N^2-palmitoyl-N^6-L-lysyl ethyl ester) oxalylamides (**N^2P/N^6Lys**), were

Received: April 22, 2019
Accepted: July 8, 2019
Published: July 18, 2019

DOI: 10.1021/acsomega.9b01086
ACS Omega 2019, 4, 12342−12356

prepared and they were found to be excellent gelators, producing transparent gels in biocompatible organic solvents such as ethyl and isopropyl esters of lauric and myristic acids, liquid paraffin, 1-decanol, and 1,2-propanediol. We have recently reported the preparation of organogels in biocompatible solvents (fatty acid ethyl and isopropyl esters of different chain lengths), and they were employed as drug carriers for a nonstereodial anti-inflammatory drug (NSAID) ibuprofen.[37] Consequently, the current study covers the investigation of the effect of the length of alkanoyl groups and solvents on gelation properties such as the minimum gelator concentration, morphology of xerogels, gel−sol transition temperatures, and gel strength. It also involves studying the drug loading and controllable release behaviors of these gelators in vitro for the transport of NSAID drug naproxen (Npx). The choice of Npx as model drug is based on its solubility in water and the relatively high UV absorbance properties. Furthermore, computational calculations were performed to understand the structural characteristics of the gel matrixes. Molecular dynamic calculations for the octamer of **N^2M/N^6Lys** in 1,2-propandiol solvent box produce valuable information regarding the structure of aggragates of the gel matrix.

2. EXPERIMENTAL SECTION

2.1. Materials. All chemicals were purchased from commercial sources (Merck, Fluka, and Sigma-Aldrich) and used without further purification if not mentioned otherwise. Lauric acid ethylester (LEE), lauric acid isoproply ester (LIE), myristic acid ethylester (MEE), and myristic acid isoproply ester (MIE) were prepared by protocols described in the literature.[38,39] The desired fatty acid isopropyl esters were obtained in high yields (88−94%) by treating the appropriate fatty acid with alcohol in large molar excess, in the presence of a catalytic amount of *p*-toluene sulfonic acid.

2.2. Techniques. The structural properties of gelators were characterized by Fourier transform infrared spectroscopy (FTIR) using Mattson 1000, ATI UNICAM machine equipped with Specac GS20730 model heating apparatus. The samples were prepared by placing the gel in KBr disks and scanned in the 4000−400 cm^{-1} range. ^1H (400 MHz) and ^{13}C (100 MHz) NMR spectra were recorded on a Bruker AV-400 High Performance Digital FT-NMR spectrometer, and chemical shifts were reported in ppm. UV−vis measurements were carried out using VARIAN UV1010M211 CARY 100 BIO UV−visible spectrophotometer. Rheological measurements were carried out with an Anton PAR MCR 301 with a cone-plate (20 mm diameter) stress-controlled rheometer. Optical rotations were measured using PerkinElmer 341 model Polarymeter apparatus. Shimatzu LC-MS 8040 was used to record mass spectra. Chemical analyses (C, H, and N) were carried out using Carlo-Erba 1108 model apparatus. Scanning electron microscopy (SEM) observations were carried out using an FEI Quanta 250 FEG field emission scanning microscope. pH measurements were carried out with a Mettler Toledo GmbH 8603 pH meter, calibrated with the standard buffers.

2.3. Synthesis. *2.3.1. Bis(N^6-L-lysyl)oxalylamide (**1**).* Oxalyl dimethyl ester, previously reported[40] (0.094 g, 0.008 mol), was added dropswise via a pressure-controlled dropping funnel to a solution of L-Lysine (2.33 g, 0.016 mol) in 50 mL of MeOH in a two-neck flask in an ice−salt bath under nitrogen. The mixture was stirred overnight at room temperature. The solvent was evaporated under vacuum, and the remaining white solid was suspended in cold diethyl ether and filtrated, affording a white solid (1.86 g, 82%). Mp decomposes at 280 °C. ^1H NMR (D_2O) δ 1.50 (m, 2H, γ-H), δ 1.61 (m, 2H, β-H), δ 1.99 (m, 2H, δ-H), δ 3.31 (t, 2H, J = 6.7 Hz, ε-H), δ 4.13 (t, 1H, J = 6.3 Hz, α-H); ^{13}C NMR (D_2O) 22.1 ppm (γ), 28.2 ppm (β), 29.8 ppm (δ), 39.5 ppm (ε), 53.2 ppm (α), 161.4 ppm (CONH), 172.3 ppm (CO_2H); IR (cm^{-1}) 3480.9, 3364.2, 3316.98, 3263.9, 3214.7, 3107.7, 3038.3, 2934.1, 2905.2, 2868.6, 1654.6, 1587.1, 1519.6, 1405.8, 1322.9, 542.8. Chemical analysis calculated for $C_{14}H_{26}N_4O_6$ (346 g mol^{-1}): C 48,54; H 7,56; N 16,17; O 27,71; found: C 48,56; H 7,59; N 16,16; O 27,70.

*2.3.2. Bis(N^6-L-lysyl ethylester)oxalylamide Hydrochloride Salt (**2**).* HCl gas was passed through the suspension of **1** (18.3 g, 0.053 mol) in ethanol (100 mL) in an ice−salt bath at 0 °C. The suspension was kept +4 °C overnight and the excess HCl was removed by passing nitrogen through the suspension for 0.5 h. The solution was concentrated by evaporating the solvent in vacuum and the remaining solid was filtered and dried in vacuum under reduced pressure for 6 h, affording 21.9 g (87%) of a white solid. Mp 175−180 °C. $[\alpha]_D^{20}$: +14.5 (CH_3CH_2OH, c:0.5). ^1H NMR (CD_3OD) δ 1.35 (t, 3H), δ 1.43−1.54 (m, 2H, γ-H), δ 1.63 (m, 2H, β-H), δ 1.90−2.00 (m, 2H, δ-H), δ 1.85 (s, 2H, NH_2), δ 3.32 (t, 2H ε-H), δ 4.05 (m, 1H, α-H), δ 4.29−4.36 (m, 2H, OCH_2); ^{13}C NMR ($CDCl_3$) 14.25 ppm (CH_3), 23.00 ppm (γ), 28.97 ppm (β), 34.34 ppm (δ), 39.45 ppm (ε), 54.28 ppm (α), 60.89 ppm (OCH_2), 159.85 ppm (CONH), 175.96 ppm (CO_2Et); IR (cm^{-1}) 3846.4, 3780.8, 3615.9, 3300.6, 3144.4, 2927.4, 2869.6, 2554.3, 1748.1, 1657.5, 1513.9, 1220.7, 1030.8, 768.5, 576.6. Chemical analysis calculated for $C_{18}H_{36}ClN_4O_6$: C 45,47; H 7,63; N 11,78; O 20,19; found: C 45,42; H 7,59; N 11,66; O 20,10.

*2.3.3. Bis(N^6-L-lysyl ethylester)oxalylamide (**3**).* Compound **2** (10.95 g, 0.023 mol) was dissolved in a small amount of water in a beaker in an ice bath and $CHCl_3$ (50 mL) was added to this mixture. Concentrated Na_2CO_3 solution was rapidly added to the solution until the pH reaches up to 10−11. The organic layer was separated and the aqueous layer was extracted a few times with chloroform. The organic layers were combined and dried on Na_2SO_4. After evaporating the solvent, a white solid was obtained, which was dried under reduced pressure (8.33 g, 90%). ^1H NMR ($CDCl_3$) δ 1.27 (t, 3H, J = 7.14 Hz), δ 1.40−1.49 (m, 2H, γ-H), δ 1.53−1.63 (m, 2H, β-H), δ 1.71−1.80 (m, 2H, δ-H), δ 1.85 (s, 2H, NH_2), δ 3.32 (t, 2H, J = 6.74 Hz, ε-H), δ 3.41 (t, 2H, α-H), δ 4.18 (t, 2H, J = 7.14 Hz, OCH_2), δ 7.55 (s, 1H, NH); ^{13}C NMR ($CDCl_3$) 14.25 ppm (CH_3), 23.00 ppm (γ), 28.97 ppm (β), 34.34 ppm (δ), 39.45 ppm (ε), 54.28 ppm (α), 60.89 ppm (OCH_2), 159.85 ppm (CONH), 175.96 ppm (CO_2Et); IR (cm^{-1}) 3447.1, 3379.7, 3316.0, 3178.1, 3148.2, 2928.4, 2882.1, 2721.1, 1745.3, 1657.5, 1518.7, 1221.7, 1070.3, 1027.9, 859.1, 768.5, 575.7. Chemical analysis calculated for $C_{18}H_{34}N_4O_6$ (402.492 g mol^{-1}): C 53,71; H 8,51; N 13,92; O 23,85; found: C 53,69; H 8,47; N 13,89; O 23,78.

2.3.4. Bis(N^2-lauroyl-N^6-L-lysyl ethylester)oxalylamide (N^2L/N^6Lys). Lauroyl chloride (0.49 g, 2.14 mmol) in chloroform (20 mL) was added dropwise via pressure-controlled funnel to a solution of compound **3** (0. 43 g, 1.07 mmol) and triethylamine (0.8 mL, 5.35 mmol) in chloroform (20 mL) in an ice bath at 0 °C. The mixture was stirred overnight at rt and water was added to the mixture. The organic layer was dried on Na_2SO_4 and evaporated in vacuum,

DOI: 10.1021/acsomega.9b01086
ACS Omega 2019, 4, 12342−12356

leaving a white solid, which was purified by column chromatography on silica gel using chloroform:EtOAc (4:1) as an eluent. The product (0.75 g, 92%) was dried in a reduced pressure for 6 h. Mp 132−134 °C. $[\alpha]_D^{20}$: +13.6 (*c*:2, $CHCl_3$). ^{1}H NMR ($CDCl_3$) δ 0.85 (t, 3H, CH_3), δ 1.25 (m, 21H), δ 1.58−1.82 (m, 6H, γ,β,δ-H), δ 2.20 (m, 2H, $COCH_2$), δ 3.27 (t, 2H, J = 6.4 Hz, ε-H), δ 4.17 (m, 2H, OCH_2), δ 4.57 (t, 1H, α-H), δ 6.19 (d, 1H, J = 7.6 Hz N^2-H), δ 7.59 (s, 1H, N^6-H). ^{13}C NMR ($CDCl_3$) 14.11 ppm (Et-CH_3), 14.17 ppm (CH_3), 22.49 ppm (CH_2), 22.68 ppm (CH_2), 25.61 ppm (CH_2), 28.78 ppm (CH_2), 29.27 ppm (CH_2), 29.34 ppm (CH_2), 29.49 ppm (CH_2), 29.61 ppm (CH_2), 29.68 ppm (CH_2), 31.90 ppm (CH_2), 32.20 ppm (CH_2), 36.61 ppm (γ), 39.32 ppm (β), 51.73 ppm ($COCH_2$), 61.51 ppm (ε), 159.84 ppm (CONH), 172.57 ppm ($COCH_2$), 172.96 ppm (CO_2Et); IR (cm^{-1}) 3284.2, 2936.1, 2858.0, 2578.4, 1746.2, 1653.7, 1526.4, 1452.2, 1365.4, 1209.2. Chemical analysis calculated for $C_{42}H_{78}N_4O_8$: C 65,75; H 10,24; N 7.30; O 16,68; found: C 65,71; H 10,19; N 7.27; O 16,59. Calculated $[m/z]$ for (N^2L/N^6Lys) 767.084 g mol^{-1} (M^+) and 790.07 for $(M + Na)^+$; found: LCMS (ESI) $[m/z]$ = 767.45 g mol^{-1} (M^+) and 789.45 $(M + Na)^+$, respectively.

2.3.5. Bis(N^2-myristoyl-N^6-L-Lysyl ethylester)oxalylamide (N^2M/N^6Lys). The reaction of **3** (0.8 g, 2.0 mmol) with myristoyl chloride (0.99 g, 4 mmol) by a similar procedure to that described for the synthesis of **N^2L/N^6Lys** produces the compound **N^2M/N^6Lys** as a white solid (1.48 g, 90%). Mp 125−127 °C. $[\alpha]_D^{20}$: +10.4 (*c*:1, $CHCl_3$). ^{1}H NMR ($CDCl_3$) δ 0.89 (t, 3H, J = 6.6 Hz CH_3), δ 1.30 (m, 25H), δ 1.58−1.71 (m, 6H, γ,β,δ-H), δ 2.24 (m, 2H, $COCH_2$), δ 3.31 (m, 2H, ε-H), δ 4.22 (m, 2H, OCH_2), δ 4.61 (q, 1H, J = 5.6 Hz α-H), δ 6.02 (d, 1H, J = 8.0 Hz N^2-H), δ 7.50 (t, 1H, J = 5.8 Hz N^6-H). ^{13}C NMR ($CDCl_3$) 14.11 ppm (Et-CH_3), 14.17 ppm (CH_3), 22.48 ppm (CH_2), 22.69 ppm (CH_2), 25.61 ppm (CH_2), 28.77 ppm (CH_2), 29.28 ppm (CH_2), 29.35 ppm (CH_2), 29.50 ppm (CH_2), 29.65 ppm (CH_2), 29.68 ppm (CH_2), 31.92 ppm (CH_2), 32.21 ppm (CH_2), 36.62 ppm (γ), 39.33 ppm (β), 51.74 ppm ($COCH_2$), 61.53 ppm (ε), 159.86 ppm (CONH), 172.58 ppm ($COCH_2$), 172.99 ppm (CO_2Et); IR (cm^{-1}) 3289.0, 2923.6, 2856.1, 1743.4, 1654.6, 1533.1, 1426.1, 1191.8, 649.9. Chemical analysis calculated for $C_{46}H_{86}N_4O_8$: C 67.11; H 10.53; N 6.80; O 15,54; found: C 67.09; H 10.47; N 6.77; O 15.46. Calculated $[m/z]$ for (**N^2M/N^6Lys**) 823.18 g mol^{-1} (M^+) and; 846.17 for $(M + Na)^+$; found: LCMS (ESI) $[m/z]$ found: 823.50 g mol^{-1} (M^+) and 845.55 $(M + Na)^+$, respectively.

2.3.6. Bis(N^2-palmitoyl-N^6-L-lysyl ethylester) oxalylamide (N^2P/N^6Lys). The reaction of **3** (0.8 g, 2.0 mmol) with palmitoyl chloride (1.043 g, 4 mmol) by a similar procedure to that described for the synthesis of **N^2L/N^6Lys** produces the compound **N^2P/N^6Lys** as a white solid (0.81 g, 92%). Mp 127−130. $[\alpha]_D^{20}$: +11.1 (*c*:1, $CHCl_3$). ^{1}H NMR ($CDCl_3$) δ 0.89 (t, 3H, CH_3), δ 1.28 (m, 29H), δ 1.55−1.89 (m, 6H, γ,β,δ-H), δ 2.21 (m, 2H, $COCH_2$), δ 3.29 (m, 2H, ε-H), δ 4.20 (q, 2H, J = 7.2 Hz OCH_2), δ 4.61 (q, 1H, J = 7.2 Hz α-H), δ 6.07 (d, 1H, J = 7.6 Hz N^2-H), δ 7.51 (t, 1H, J = 6.0 Hz N^6-H). ^{13}C NMR ($CDCl_3$) 14.11 ppm (Et-CH_3), 14.17 ppm (CH_3), 22.49 ppm (CH_2), 22.68 ppm (CH_2), 25.61 ppm (CH_2), 25.88 ppm (CH_2), 28.44 (CH_2), 28.78 ppm (CH_2), 29.28 ppm (CH_2), 29.35 ppm (CH_2), 29.50 ppm (CH_2), 29.65 ppm (CH_2), 29.69 ppm (CH_2), 31.92 ppm (CH_2), 32.19 ppm (CH_2), 36.60 ppm (γ), 38.86 ppm (δ), 39.32 ppm (β), 51.65 ppm (α), 51.73 ppm ($COCH_2$), 61.50 ppm (ε), 159.84 ppm (CONH), 172.57 ppm ($COCH_2$), 172.97 ppm (CO_2Et); IR 3292.8, 2923.5, 2855.1, 1742.3, 1652.7, 1528.3, 1463.7, 1375.0, 1191.8, 1028.8, 869.7, 723.1. Chemical analysis calculated for $C_{50}H_{94}N_4O_8$ (879.60g mol^{-1}): C 68.29; H 10.77; N 6.37; O 14.55; found: C 68,31; H 10.66; N 6.29; O 14.49. Calculated $[m/z]$ for (**N^2P/N^6Lys**) 879.29 g mol^{-1} (M^+) and 901.49 for $(M + Na)^+$; found: LCMS (ESI) $[m/z]$ = 879.60 g mol^{-1} (M^+) and 901.60 $(M + Na)^+$, respectively.

2.4. Gelation Studies. *2.4.1. Preparation of the Organogels.* Required amounts of the compounds in 1 mL of organic solvent were placed in a screw-capped tube with an internal diameter (i.d.) of 10 mm and slowly heated until the solid was completely dissolved. Then, the solutions were cooled (undisturbed) to room temperature. After 1 h, colorless and transparent gels were obtained. They were assessed as stable by inversion of the glass tube.

2.4.2. Determination of the Minimum Gel Concentration (MGC). The gelation test was carried out by following the procedure mentioned in the literature.[41] A gelator (1 mg) was dissolved in 1 mL of an organic solvent. The mixture was heated up to a temperature of 20 °C below the boiling point of the solvent until the gelator has completely been dissolved. Then, the solution was allowed to stand in a thermostated water bath at 25 °C. After about 15 min, it was checked if the solution was gelled, if not, then 1 mg of more gelator was added and the procedure was repeated until the gelation occurs. The concentration where the gelation occurs is recorded as the minimum gelation concentration (MGC) (mg/mL). In the case when 1 mg of the gelator could not be dissolved in 1 mL of the specified solvent, this was reported as the gelator is not soluble in this specific solvent. On the other hand, if the gelator is soluble in over 10% of the specific solvent, then the gelator was referred as soluble in this specific solvent.

2.4.3. Determination of Gel−Sol Transition Temperature (T_g). The gel prepared in 1 mL of organic solvent in a test tube with internal diameter (i.d.) of 10 mm was kept at 25 °C for 6 h. All of the glass tubes having standard dimension of 12 mm × 75 mm were used and a steel ball with a weight of 0.25 g was carefully placed on the surface of the gel in this tube in an oil bath with a temperature controller. The bath was heated at 1 °C intervals until the ball falls down the bottom of the tube, which corresponds to the melting point (gel−sol transition temperature) (T_g) of the gelator. This ensures that stress generated by the gel on the measurement of its melting point is approximately constant in each case. This procedure was repeated with different concentrations of gelators.[42]

2.4.4. Microscopy Studies. The reprecipitation approach was followed in the preparation of samples for SEM analyses since the dried samples were prepared by the deposition method,[43] where the deposition of a gel sample followed by drying in vacuum is too difficult to handle because of the high boiling point of solvents. This concurrently causes the deformation of xerogels. So, xerogels were prepared by following a previously reported method.[43] A quick precipitation of gels from organic fluids in hexane is very useful for sample preparation, where their nanoscaled network is still maintained by the quick precipitation. The samples were prepared by rapid stirring of the gel obtained from organic fluids either with a magnet or a vortex followed by addition of hexane. Gelators were participated as fibers, and the solvent was removed via a Pasteur pipette. Centrifugation (6000 rpm) was applied to the cases where the separation of the layers is

DOI: 10.1021/acsomega.9b01086
ACS Omega 2019, 4, 12342−12356

not good enough. The addition and separation of hexane were repeated until all high-boiling-point fluids have been washed away. The excess of hexane was removed by freeze-drying for 24 h.

2.4.5. Determination of Gel−Sol Transition Enthalpy (ΔH_m). The enthalpy of gel−sol transition was determined using the van't Hoff equation (eq 1.)[44,45] by plotting ln [C_m] versus $1/T_g$, where C_m corresponds to the concentration of gelator as mol L^{-1}, T_g corresponds to the phase-transition temperature, and R corresponds to the Rydberg gas constant (R = 8.314 J mol^{-1} K^{-1})

$$d \ln[C_m]/d(1/T_g) = -\Delta H_{sol}/R \quad (1)$$

2.4.6. Rheology Measurements. The viscoelastic properties of the gels obtained from **N^2L/N^6Lys**, **N^2M/N^6Lys**, and **N^2P/N^6Lys** gelators in liquid paraffin and 1-decanol were measured by a 20 mm cone-plate stress-controlled rheometer (Anton PAR MCR 301) at a constant shear stress (1.3 Pa) and at 25 °C. The width of the gap was 0.047 mm. Oscillatory amplitude sweep experiments (γ: 0.01−100%) were carried out at a fixed frequency of 10 rad s^{-1}, to determine the linear viscoelastic (LVE) range and the crossover point of the gels ($G'' > G'$). The samples were prepared the day before the analysis and left overnight at a controlled temperature of 25 °C to complete the gelation process. The set sample was placed on the plain sample surface of the rheometer. After establishing the LVE of each organogel, frequency sweep tests were performed at a constant shear stress within the LVE region of each sample. Then, the experiment was done in frequency sweep modes with 1% strain.

2.5. Computational Modeling. The monomer composed of alkanoyl, oxalyl, and lysine was optimized using AM1[46] by Gaussain 03.[47] Assisted Model Building with Energy Refinement (AMBER version 11) was used for the molecular dynamic calculations.[48] Atomic charges were derived by antechamber as implemented in AMBER, and they were corrected for the equivalent atoms.[49] ff99SB[50] library was employed for the atom types and parameter/topology. The angle parameters for N−C−C backbone in oxylyl linkage were adopted from the general amber force field (GAFF) library.[51] Xleap as implemented in AMBER was used to derive library for the components of the monomer and to solvate the tetramer and polymeric forms of the gelator as well as to form parameter/topology and coordinate files. The octamer form of the gelator was contracted by Discovery Studio Visulazer 4.1[52] using the minimized monomer and followed by AM1 calculation to minimize the aggregate. Then, the individual coordinates in the minimized octamer were used for the molecular dynamic calculations. 1,2-Propanediol was also minimized by AM1, and charges for each of its atoms were derived by antechamber. A solvent box (PRPPBOX) was derived from this molecule composed of 20 molecules. Xleap was used to prepare the octamer in 1,2-propanediol. Systems were minimized in two steps. In the first step, the gelator molecules were kept fixed; only 1,2-propandiol molecules were allowed to move. In the second step, all of the atoms were allowed to move. In both steps, calculations were performed in 5000 steps: 2500 steps with the steepest descent method and 2500 steps with the conjugate gradient method. Heating was performed in the canonical ensemble for 200 ps, where the aggregates of gelator were restrained with a force constant of 10 kcal mol^{-1} $Å^{-2}$. Equilibration was performed for 17.5 ns in a canonical ensemble at a temperature of 300 K and a pressure of 1 atm. The step size was 2 fs during the entire simulation. A Langevin thermostat and barostat were used to couple the temperature and pressure. The SHAKE algorithm was applied to constrain all bonds containing hydrogen atoms.[53] The nonbonded cutoff was kept at 10 Å, and long-range electrostatic interactions were treated using the particle-mesh Ewald (PME)[54] method with a fast Fourier transform grid with a spacing of approximately 0.1 nm. Cluster analyses were done using Chimera UCSF,[55] which is also used for the visualization of molecular dynamic trajactories. Ptraj module as implemented in AMBER was used to calculate RMSD changes, hydrogen-bond analyses, and radial distribution function (RDF).[56] The graphical outcomes of all of these analyses were represented by GraphPad Pris 4.

2.6. Drug Loading and Release. *2.6.1. Drug Loading.* Loading of Npx into the gel network was carried out by the following procedure as described in the literature.[37] This involves heating a mixture of the drug (3.0 mg), the solvent (1.0 mL), and the gelator (4.0 mg) in a septum-capped tube with an internal diameter of 10 mm; the mixture was heated in an oil bath to a temperature of 20 °C below the boiling point of the solvent until achieving a homogenous solution, followed by cooling the solution to 25 °C and kept it undisturbed at this temperature for about 6 h to ensure that the gelation occurs, observed by the stability of the mixture by inversion of the glass tube.

The drug loading capacities of gelators were obtained by a slow successive addition of Npx to the prepared gels (on the gelators MGC 6.0 mg) in different solvents (1 mL) until the gel structures are reproduced. The maximum drug loading capacity (MDLC) of gelators was found from the following equation (eq 2)

$$\text{MDLC} = \%w_d/w_g \times 100 \quad (2)$$

where w_d is the weight of drug loaded in the gel and w_g is the weight of gelator in the gel matrix.

2.6.2. Drug Release. The Higuchi equation (eq 3) was employed to quantify drug release from organogels into artificial physiological fluid. This equation provides possibilities both to facilitate device optimization and to better understand the underlying drug release mechanisms.[57]

$$M_t/M_\infty = kt^{1/2} \quad (3)$$

where M_t is the cumulative absolute amount of drug released at time t, M_∞ is the cumulative absolute amount of drug released at infinite time, k is a constant reflecting the design variables of the system, and t is the time.

UV−vis spectroscopy was used to determine the amount of drug released. UV−vis scanning indicates that Npx has a maximum UV absorption wavelength at 262 nm where the gelators have no absorption. For a typical drug release experiment, 6 mL of buffer (0.1 M phosphate) was placed on the top of the drug loaded gel in glass tube as described above in a thermostated bath at 25 °C. With time intervals of 1 h for a period of 9 h, 3 mL of sample was taken from the buffered solution and the amount of the drug released was determined by UV. Fresh buffered solution (3 mL) was added to maintain the initial amount of 6 mL of buffered solution. This procedure was followed to see the effect of solvent, pH (pH 5.0, 7.0, and 7.4), concentration of Npx, and gelators on the release rate. The effect of Npx concentration (0.5−5 mg) on the cumulative release was measured from **N^2M/N^6Lys** (4.0

DOI: 10.1021/acsomega.9b01086
ACS Omega 2019, 4, 12342−12356

Scheme 1. Organogelators Prepared in This Study[a]

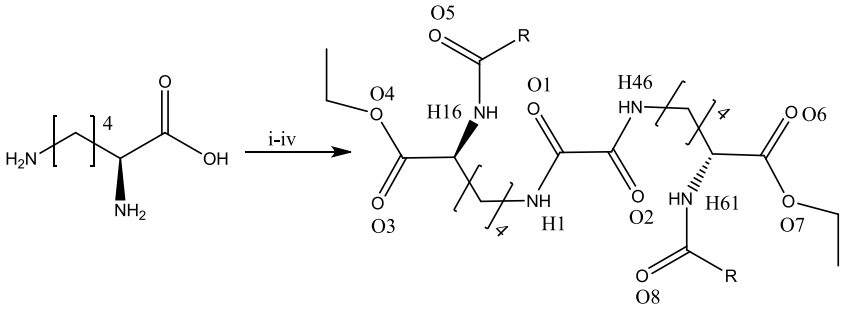

[a](i) Dimethyl Oxalate; (ii) HCl/EtOH; (iii) $Na_2CO_3/CHCl_3$; (iv) RCOCl. R = $C_{11}H_{23}$ (**N^2L/N^6Lys**), R = $C_{13}H_{27}$ (**N^2M/N^6Lys**), and R = $C_{15}H_{29}$ (**N^2P/N^6Lys**).

Table 1. Minimum Gel Concentration (MGC, mg/mL) of L-Lysine-Based Gelators Prepared in Various Solvents

	MIE	MEE	LIE	LEE	1,2-propandiol	1-decanol	paraffin
N^2L/N^6Lys	6	6	4	4	4	6	6
N^2M/N^6Lys	4	4	4	4	6	6	4
N^2P/N^6Lys	4	4	4	4	4	4	6

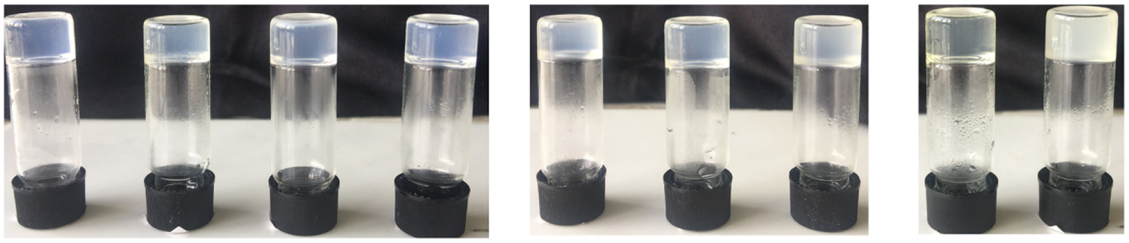

Figure 1. Images of gels at MGC. From left: **N^2M/N^6Lys** in 1-decanol, MIE, LEE, and liquid paraffin; **N^2L/N^6Lys** in 1-decanol, MIE, and LEE; **N^2P/N^6Lys** in 1-decanol and MIE.

mg) gel in liquid paraffin (1.0 mL) at pH 7.4 (0.1 M phosphate buffer) and 25 °C since the drug cumulative release quantity was low in this gel. **N^2P/N^6Lys** showed the highest drug loading capacity in all of the tested fluids. Hence, the effect of solvent on the drug release was measured with this gelator. The gel forms of **N^2P/N^6Lys** (6 mg) containing Npx (3 mg) are prepared in 1 mL of four different solvents (LEE, 1-decanol, 1,2-propandiol, and liquid paraffin) and the release rate of Npx into 6 mL of the buffered solution (0.1 M phosphate) at pH 7.4 and 25 °C was measured. The effect of pH (at three different pH values: 5.0, 7.0, and 7.4) on the release of Npx was studied in LEE since the highest release is observed (40% within 24 h) in this solvent. The effect of concentration of gelators on cumulative release of Npx (3 mg) in liquid paraffin was studied at two different gel concentrations (4 and 6 mg) at pH 7.4 (0.1 M phosphate buffer) and 25 °C. For all of the measurements, each point represents the mean value ± SD (n = 3).

3. RESULTS AND DISCUSSION

3.1. Synthesis. The synthesis and applications of biocompatible L-lysine-based LMWOGs have widely been reported.[58] They are generally linked via N^2 end to form C_2 symmetric structures. The current work involves the synthesis of L-lysine-based LMWOG via the selective N^6 linkage using oxalyl as a linker. Moreover, lauric, myristoic, and palmitoic acid chlorides were used to acylate L-lysine at the N^2 end to produce three different gelators bearing hydrophobic site chains with different lengths. These organogelators, **N^2L/N^6Lys**, **N^2M/ N^6Lys**, and **N^2P/N^6Lys**, are composed of residues from natural resources and prepared with high yield by facile synthetic paths (Scheme 1), which were fully characterized by Fourier transform infrared (FT-IR), NMR, and mass spectrometry techniques.

3.2. Gelation and Gel Properties. The gel formation of these gelators (**N^2L/N^6Lys**, **N^2M/ N^6Lys**, and **N^2P/N^6Lys**) was studied in common cosmetic solvents such as LEE, LIE, MEE, MIE, 1,2-propandiol, and 1-decanol. It was found that they all form gel in these solvents with MGCs in the range of 4–6 mg/mL (Table 1), mostly possessing a transparent appearance (Figure 1). They provide a system prepared from natural sources, which could be used for the drug delivery/release applications.

The gel–sol transition temperature (T_g) offers useful information regarding the stability of the gels. The data obtained for concentration-dependent T_g of each gelator in different solvents (1 mL) are presented in the Supporting Information (Tables S1–S7). They indicate that increasing the concentration of the gelator increases the thermal stability of the gels (Figure 2). The highest T_g values are obtained for the gels in liquid paraffin even at lower concentrations (Table S3). This may be attributed to the fact that the intermolecular hydrogen bonds are stronger in this solvent compared to the rest. It is expected that hydrophilic solvents such as 1-decanol and 1,2-propanediol would have competition to form hydrogen bonds with the gelator, thus weakening the intermolecular interactions between the gelator molecules (Figure S21 and Table S2). Besides, T_g's for these hydrophilic gels are low,

DOI: 10.1021/acsomega.9b01086
ACS Omega 2019, 4, 12342–12356

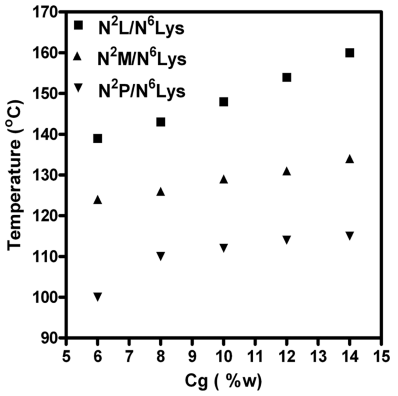

Figure 2. Plot of T_g versus the weight of gelators C_g (% w) in liquid paraffin.

indicating that the drug loading temperature is comparable to body temperature, which prohibits the racemization of chiral drugs, during loading processes.

The key role of intermolecular hydrogen bonds in the formation of these gels was qualitatively identified by FT-IR analyses. Temperature-dependent (25−110 °C) IR spectrum of **N²M/N⁶Lys** with T_g of 104 °C in MIE is displayed in Figure 3. It demonstrates that there are hydrogen bonds involving NH and C═O in the gel. These intermolecular interactions disappear at 110 °C, corresponding to the temperature above the gel−sol transition. The bands corresponding to the NH stretching at 3288 and 3325 cm^{-1} at lower temperatures below T_g are shifted to 3350 and 3400 cm^{-1} at the temperature above T_g (110 °C). This clearly demonstrates the involvement of NH functions via the hydrogen bonds in maintaining the 3D structure of the gel (Figure 3, right). A similar pattern was found for the C═O stretching: the possible intermolecular interactions indicated by C═O stretching appearing at 1650 (amide I) and 1530 (amide II) cm^{-1} are shifted to 1693 and 1501 cm^{-1}, respectively, in the free form at 110 °C (Figure 3, left).

Temperature-dependent IR spectrum of **N²M/N⁶Lys** with T_g of 124 °C in liquid paraffin is displayed in Figure 4. A similar observation obtained for the spectra in MIE was also seen for this gelator in paraffin (Figure 4). The hydrogen bonds between NH and C═O in the gel are represented by the NH stretching at 3284 at lower temperatures, below T_g (Figure 4, right). This peak is shifted to 3400 cm^{-1} at the temperature above the gel−sol transition (Figure 4, right). This shift is a clear indication of the disappearance of the intermolecular hydrogen bonds. The peak corresponding to the C═O stretching at 1650 (amide I) and 1530 (amide II) cm^{-1} are shifted to 1690 and 1500 cm^{-1} at 130 °C (Figure 4, left). Similarly, this indicates that carbonyl functions are involved in the intermolecular interaction in the gels for the formation of the matrix.

It is known that gels spontaneously self-aggregate to form a 3D network structure via entwined nanofibers,[59] which can be observed by electron microscopy. The preparation of samples for SEM analyses involves drying samples in vacuum following deposition of solvents from gel samples. Unfortunately, the solvents used in the preparation of the gels in the present study have higher boiling points, which hampers the direct preparation of xerogels by the freeze-drying technique for SEM analyses. Thus, the reprecipitation procedure was employed for the preparation of samples.[43] The nanoscale network structures of the gels remain unchanged by shaking the samples with hexane. However, this may cause the deformation of xerogel form. The SEM images of **N²L/N⁶Lys**, **N²M/N⁶Lys**, and **N²P/N⁶Lys** are presented in Figure 5. They indicate that the solvents and the chain length of alkanoyl parts in the gelators influence the morphology of xerogels (Figure 5). The xerogel of **N²L/N⁶Lys** seems to be self-assembled in a cross-linked and entangled manner in liquid paraffin compared to that in 1-decanol. This may be associated with the different hydrogen-bond patterns in different solvents. The gels in liquid paraffin have probably stronger hydrogen-bond network compared to those in 1-decanol. The structure with the shortest alkanoyl site arms (**N²L/N⁶Lys**) has an entangled string appearance in liquid paraffin, while it produces rather a smooth stringlike pattern in 1-decanol. On the other hand, medium-sized **N²M/N⁶Lys** has a flat and thicker fiber structure than **N²L/N⁶Lys** in 1-decanol. The gel with the longest arm chain (**N²P/N⁶Lys**) gives a spongelike pattern in liquid paraffin. So, hydrogen bonds, as expected, are key players in the self-aggregation process of the gelation, but the

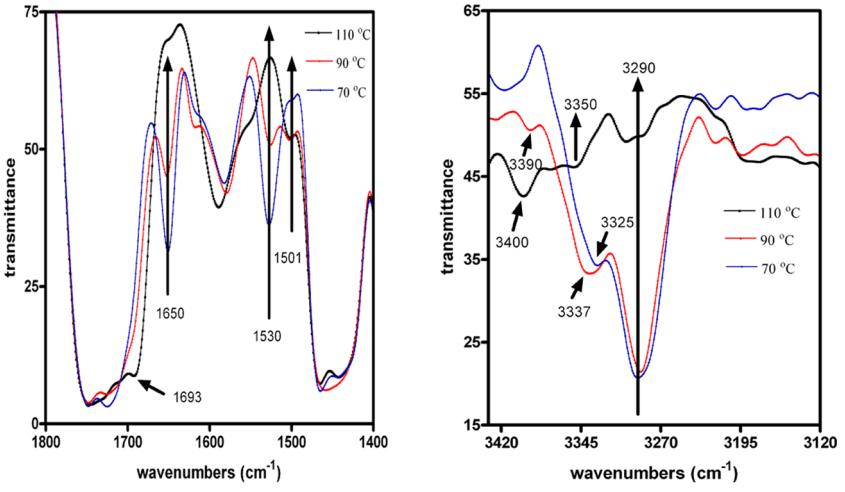

Figure 3. Temperature-dependent IR spectra corresponding to C═O (left) and NH (right) stretching bands for gelator **N²M/N⁶Lys** (12 mg) in 1 mL of MIE.

DOI: 10.1021/acsomega.9b01086
ACS Omega 2019, 4, 12342−12356

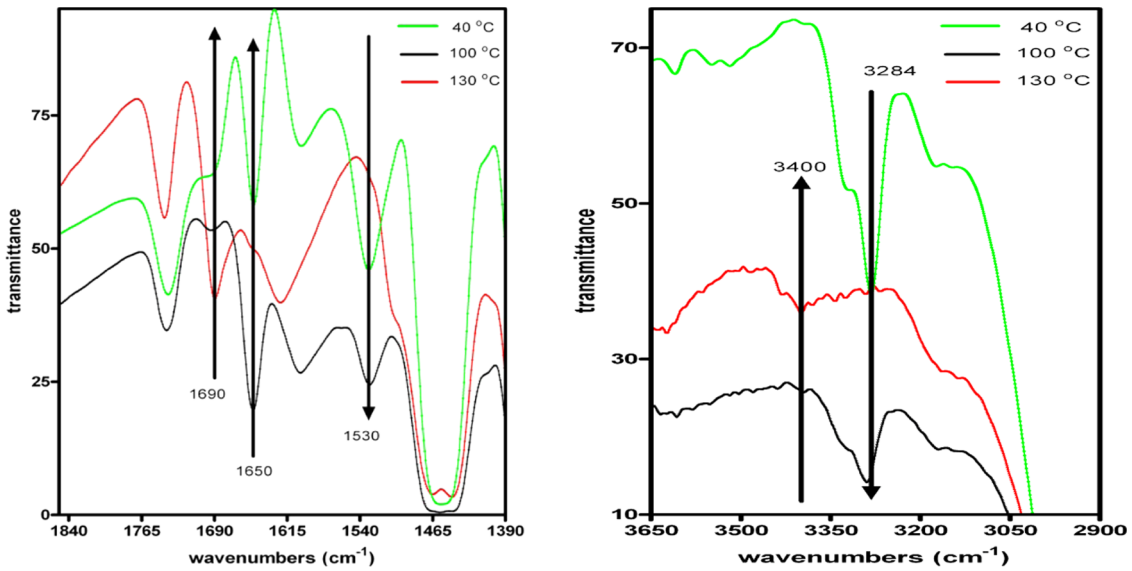

Figure 4. Temperature-dependent (25−130 °C) IR spectra corresponding to C═O (left) and NH (right) stretching bands for gelator **N²M/N⁶Lys** (8 mg) in 1 mL of liquid paraffin.

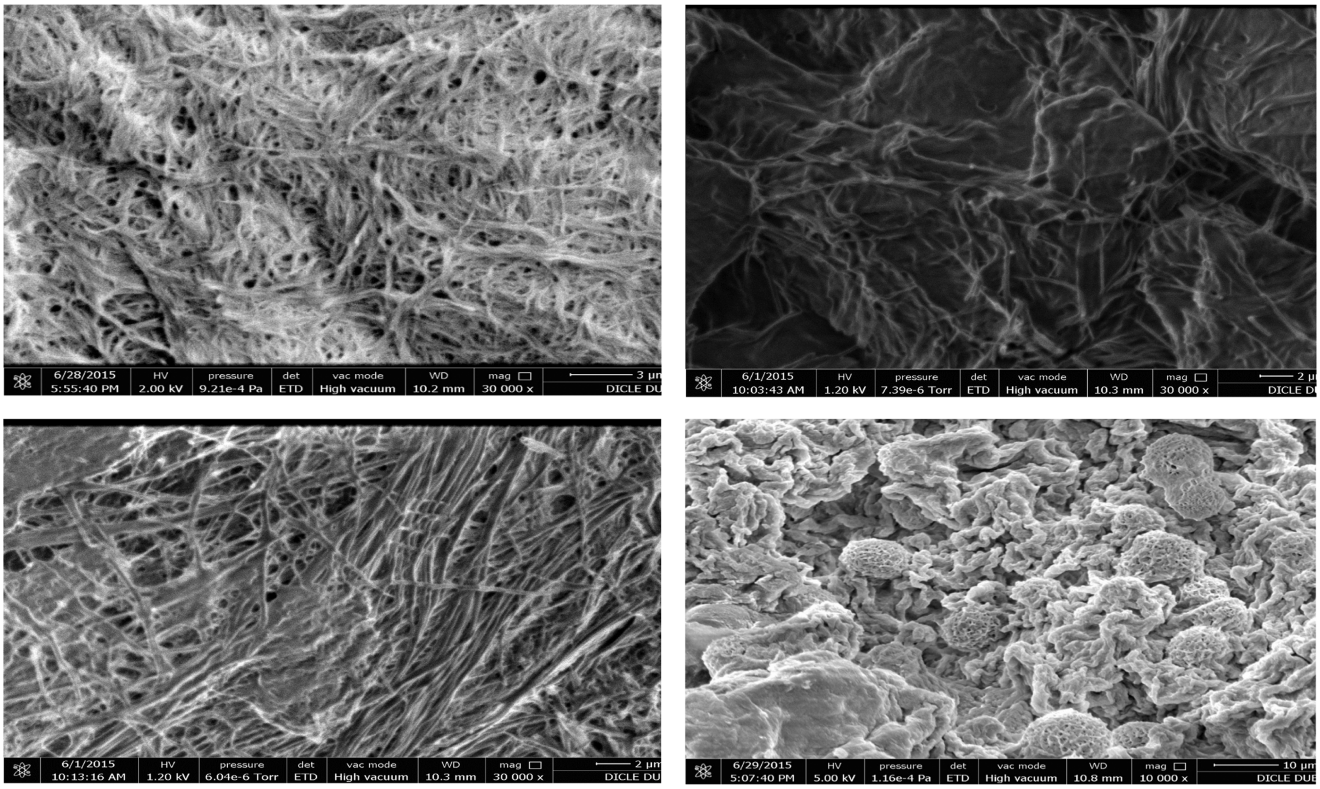

Figure 5. SEM images of xerogels. (Left top) **N²L/N⁶Lys** (8 mg) in 1 mL of liquid paraffin, (right top) **N²L/N⁶Lys** (6 mg) in 1 mL of 1-decanol, scale bars = 3 and 2 μm, respectively; (left bottom) **N²M/N⁶Lys** (6 mg) 1 mL of 1-decanol, (right bottom) **N²P/N⁶Lys** (6 mg) in 1 mL of liquid paraffin, scale bars = 2 and 10 μm, respectively.

alkanoyl groups appear also to play a significant role in the formation of nanostructures of these gels.

Determination of physical properties of gels is important for the prediction of their specific role in many applications, particularly thermodynamic parameters are of great importance. For example, the van't Hoff equation (eq 1) may be used to calculate the gel−sol transition enthalpy if the gel−sol transition is comparable to the melting of crystals.[44,45] The gelation enthalpies obtained from eq 1 by plotting ln $[C_m]$ vs $1/T_g$ (see Figures S3−S9 in the Supporting Information) for three gelators in different solvents are given in Table 2.

The effect of solvents on the gel−sol transition enthalpy (ΔH_{sol}) is summarized in Table 2, where ΔH_{sol} is roughly considered as ΔH in the van't Hoff equation. However, it is very difficult to make a straightforward statement about the influence of the solvent on the thermal stability of the gels. On the other hand, it is clear that **N²M/N⁶Lys** possesses lower stability almost in all solvents, except in LEE and 1-decanol

DOI: 10.1021/acsomega.9b01086
ACS Omega 2019, 4, 12342−12356

Table 2. Gel−Sol Transition Enthalpies (ΔH_{sol}, kJ mol^{-1}) Calculated from van't Hoff Equation (eq 1)

	ΔH_{sol} (kJ mol^{-1})		
solvents	N^2L/N^6Lys	N^2M/N^6Lys	N^2P/N^6Lys
MIE	41.7	149.6	49.4
MEE	46.0	61.0	33.7
LIE	68.7	90.5	53.9
LEE	187.4	112.6	46.2
liquid paraffin	78.1	130.3	80
1-decanol	37.8	78.2	93.2
1,2-propandiol	100.6	109.7	73.8

and **N^2P/N^6Lys** have higher stability in almost all solvents, except in MIE and 1-decanol (comparable stability to N^2P/N^6Lys in paraffin (80 vs 78.1 kJ mol^{-1}).

Moreover, enthalpies for the gels in LEE and 1-decanol offer a reasonable order to correlate the stability of gels with the polarity of solvents and the length of site arms, namely, lauroyl, myristoyl, and palmitoyl. As the length increases, the stability decreases in 1-decanol, whereas the order is reversed in LEE (Table 2). So, there is a critical point in the thermal stability of gels governed by a balance between the polarity of the solvent and the hydrophilicity of the gelator.

The rheological behavior of the gels in liquid paraffin and 1-decanol are represented in Figure 6. For all of the organogels tested, the storage modulus (G') was higher than the loss modulus (G'') over the frequency ranges at 1% strain (lower than the yield strain) (Table 3). This produces smaller values of G''/G', which corresponds to the loss factor, defined as tan δ (tan $\delta = G''/G'$), an indication of the elastic nature of the gels. Hence, all of the gels show elastic nature. This may be considered as a measure of the consistency parameter for dermal and transdermal applications, which is important for the drug-resident period on the application region and drug absorption via skin and drug release.[60]

There are two other rheological parameters for the description of the gel properties, which are important indicators for their drug carrier properties in the dermal and topical applications. These are the complex viscosity η^* ($\eta^* = G^*/\omega$) and complex modulus G^* ($G^* = G' + G''$). The former is defined as the total resistance of the network structure against the applied strain, while the latter represents the energy involved in the interactions between the network elements.[61] The lower η^* means a thinner layer of semisolid, which indicates that the gels with optimal low values of η^* could be applied to the skin, resulting in more rapid absorption of drug.[62] Data demonstrate that all of the gel systems possess reliable viscous properties but **N^2M/N^6Lys**/liquid paraffin and **N^2L/N^6Lys**/1-decanol have more viscous nature, and therefore this gelator in both fluids produce sufficiently stable organogels with moderate energy (Table 3). And consequently, **N^2P/N^6Lys**/1-decanol and **N^2P/N^6Lys**/liquid paraffin systems may be regarded as better candidates of drug carries.

3.3. Computational Modeling. As far as our current knowledge of the literature is concerned, there are a few reports on the computational modeling of gel structure.[63−65] Although the gel structures are thought to be compact organizations, it is important to know about their structural properties and their interaction pattern with the solvent. Here, we report a detailed computational calculation, including semiempiric and molecular dynamic calculations, for the octomer of **N^2M/N^6Lys**. The octomer was constructed from a minimized monomer at AM1 level by considering as much as possible intermolecular hydrogen-bond interactions. The minimized octamer indicates that the oxalate-lysine backbone tends to bend, producing a spiral structure with a DNA-like pattern where alkyl long chains line up in a parallel manner (Figure 7). It also demonstrates that apart from the oxalate residue, alkanoyl-lysine amides are involved in the interactions, whereas the ester functions lie outside of the frame. This is consistent with the experimental observations by IR. Potential energy of the system as a function of time during MD for a period of 17.5 ns at 300 K and the RMSD of the octamer during the same MD calculations compared to its starting coordinates are presented in Figure 8. The energy change indicates the conversion of the system to a reasonable level, and RMSD changes demonstrate that the system has achieved an acceptable equilibrium state.

The calculations performed in the solvent box of 1,2-propandiol for the octomer of the gelator (**N^2M/N^6Lys**) provide very interesting structural information for the aggregation phenomena of the gelation. The results demonstrated that the bended octamer structure is maintained during the molecular dynamic simulation (Figure 9). Hydrogen-bond analyses between donors and acceptors are presented in Table 4. They display that the average hydrogen bonds between the oxalyl functions (**Hbond4** and **Hbond5**) are relatively shorter, and hence they are thought to be the main driving forces for maintaining the 3D structure of the gels. On the other hand, the amide hydrogen of myristoyl tends to form hydrogen bonds with its carbonyl counterpart (**Hbond1** and **Hbond4**) rather than with the ester functions (**Hbond2** and **Hbond5**) since the latters have larger average bond distances. This is consistent with the experimental observations by FTIR as mentioned earlier. The other significant outcome is the calculation of radial distribution functions (RDFs)[56] from molecular dynamic trajectories. It provides data to give the probability of finding a particle in the distance from another particle. The distances between the acceptors in the solvent and potential donors (O6, O7, and O8 in Scheme 1) in the gelator are calculated (Figure 10). They show the density distribution of the solvent acceptors around three oxygens in the octamer. This means that it is more likely that the solvent molecules would be in contact with the gelator at around 2.5 Å.

3.4. In Vitro Drug Study. *3.4.1. Drug Loading Capacity of Gelators.* To relatively compare the maximum drug loading capacity of the gels, the same amount of the gelator (6 mg) was employed in all applications. The calculated maximum amounts of Npx encapsulated by gelators prepared in different solvents are given in Table 5. The relatively higher capacity displayed by **N^2P/N^6Lys** and **N^2M/N^6Lys** in all solvents may be associated with their longer chain length on the N^2-lysine amino group. It seems somehow the polarity of the solvent also influences the loading capacity, the more polar the lower capacity (Table 5). The loading of Npx into the gel network was studied by UV−vis spectroscopy, as described in the Materials section. An image of Npx (3.0 mg) loaded **N^2M/N^6Lys** in liquid paraffin is demonstrated in Figure 11.

3.4.2. Drug Release. It is mainly possible to apply a mathematical equation for the description of the time-dependent release of drugs. This offers a very useful way for the prediction of the kinetics of the release. There are many mathematical models to design a number of simple and complex drug delivery systems. They also predict the overall

DOI: 10.1021/acsomega.9b01086
ACS Omega 2019, 4, 12342−12356

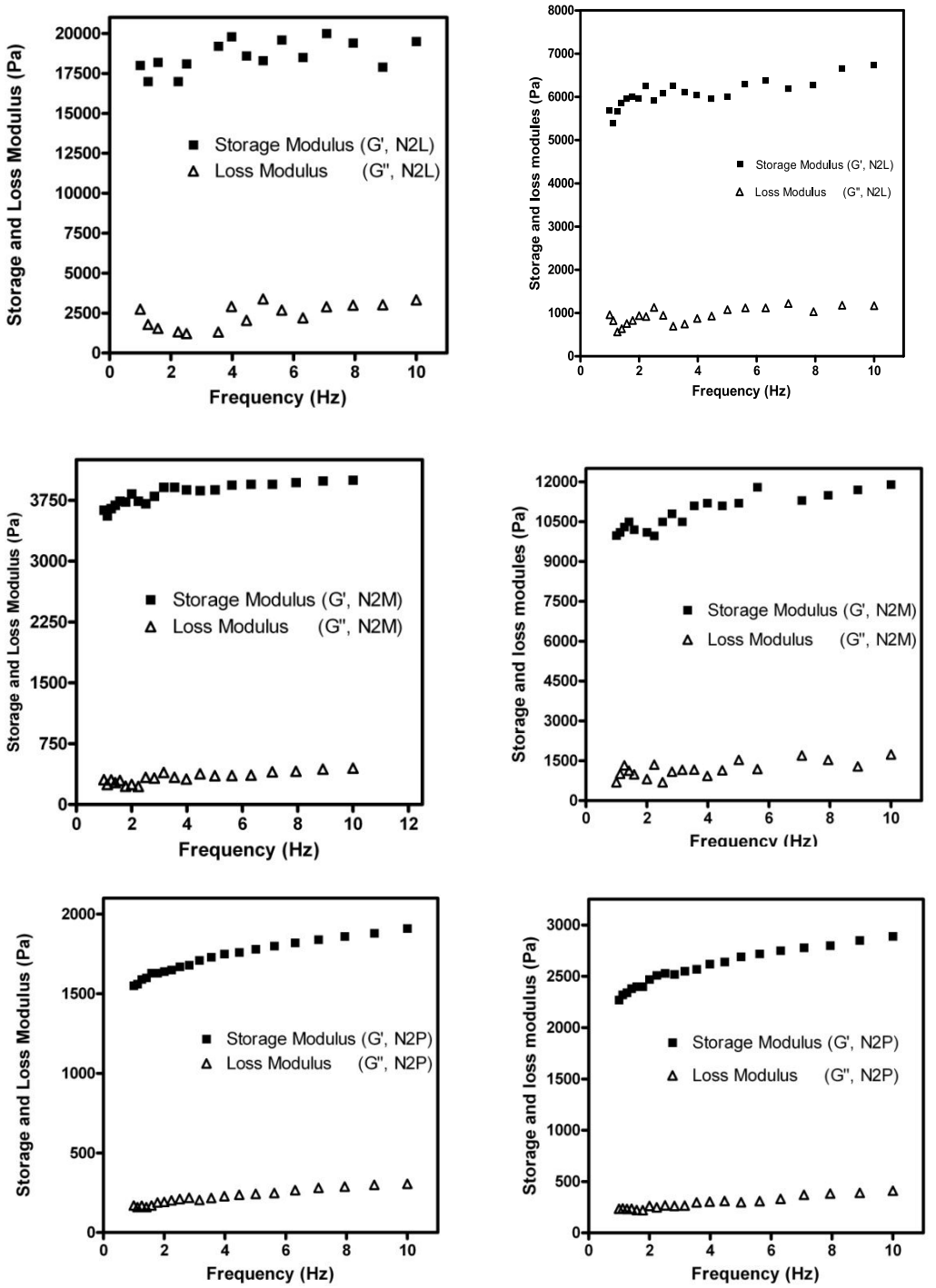

Figure 6. Storage (G', solid square) and loss moduli (G'', solid triangle) for the gels of **N^2L/N^6Lys** prepared in liquid paraffin and 1-decanol as a function of frequency at 25 °C; (top left) in 1-decanol, (top right) in liquid paraffin, (middle left) in 1-decanol, (middle right) in liquid paraffin, (bottom left) in 1-decanol, and (bottom right) in liquid paraffin. The analyses were performed on the gels about 20 h after the gelation. All samples were prepared above MGC (8 mg/mL).

Table 3. Rheology Data Taken at 3.55 Hz for Organogels in Liquid Paraffin (8 mg/mL) and 1-Decanol (8 mg/mL)

gelators	solvent	G' (Pa)	G'' (Pa)	tan δ	η^*	G^*
N^2L/N^6Lys	liquid paraffin	6110	939	0.153	276	6856
N^2M/N^6Lys	liquid paraffin	11 100	1170	0.105	501	12 270
N^2P/N^6Lys	liquid paraffin	2570	297	0.115	116	2867
N^2L/N^6Lys	1-decanol	19 800	2580	0.13	802	20 510
N^2M/N^6Lys	1-decanol	3880	335	0.086	176	4245
N^2P/N^6Lys	1-decanol	1730	217	0.125	78	1947

DOI: 10.1021/acsomega.9b01086
ACS Omega 2019, 4, 12342−12356

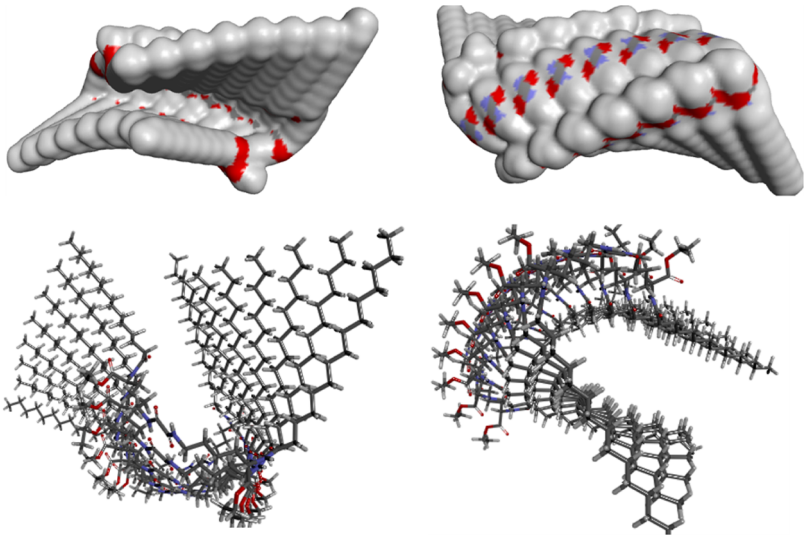

Figure 7. AM1-minimized structure of octamer of N^2M/N^6Lys.

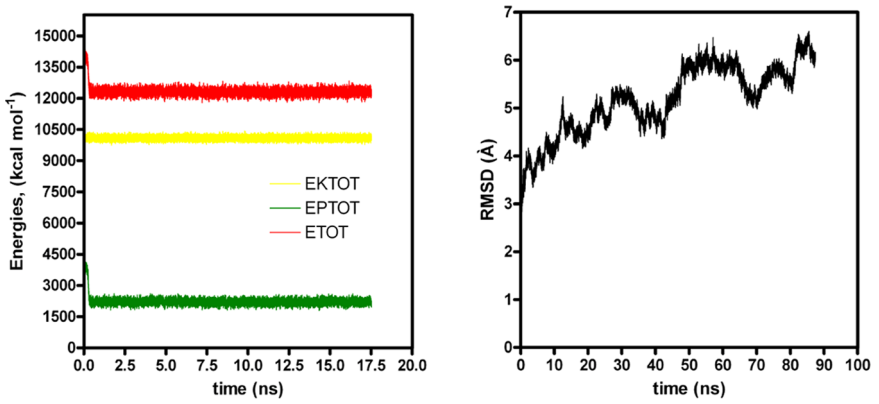

Figure 8. (Left) Energies of the system as a function of time during MD for a period of 17.5 ns at 300 K and (right) RMSD of the octamer during the same MD simulations, compared to its starting coordinates.

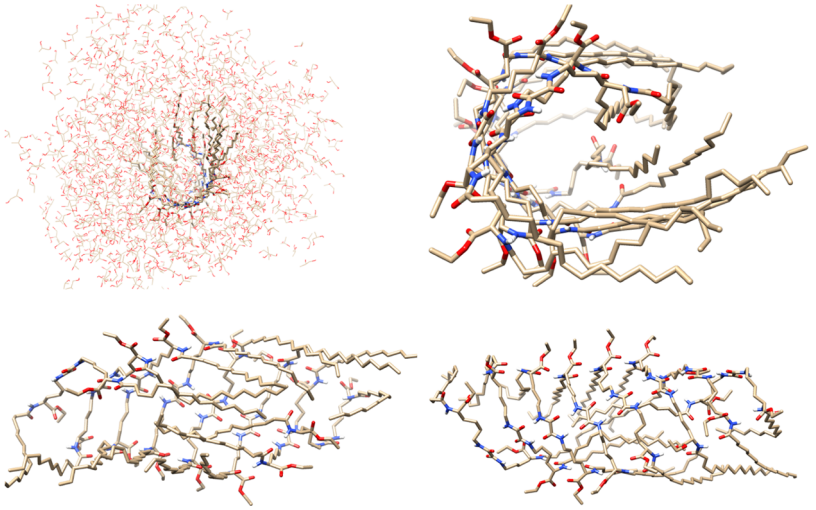

Figure 9. The last trajectory of the gelator in 1,2-propandiol and the cluster with the higher population in three different views. Hydrogens are omitted for clarity.

release behavior.[57,66,67] The first mathematical model known as the Higuchi equation proposed to explain the release of a drug from matrix systems.[57,57] This equation is the most common mathematical model for the description of the release rate of drugs from matrix systems. In our study, the linear responses of the cumulative release amounts against the square root of time demonstrated that the release of Npx from the gels followed the Higuchi equation and matrix diffusion kinetics with a

DOI: 10.1021/acsomega.9b01086
ACS Omega 2019, 4, 12342−12356

Table 4. Average hydrogen-bond distances (Å) between the acceptors and donors involved in the formation of 3D structure of the gel obtained from the MD calculations[a]

residues	HBond1	HBond2	HBond3	HBond4	HBond5	HBond6
1−2	2.999 ± 1.1670	4.328 ± 1.374	2.175 ± 0.536	2.171 ± 0.591	3.233 ± 2.079	3.686 ± 0.978
2−3	2.086 ± 0.378	3.690 ± 0.809	2.024 ± 0.230	1.983 ± 0.191	2.201 ± 0.584	3.446 ± 0.820
3−4	2.162 ± 0.544	3.452 ± 0.728	2.005 ± 0.181	1.960 ± 0.165	2.020 ± 0.276	3.535 ± 0.729
4−5	2.604 ± 1.205	3.079 ± 0.816	2.074 ± 0.299	1.999 ± 0.205	3.498 ± 0.901	2.441 ± 0.712
5−6	2.607 ± 0.984	3.270 ± 0.813	1.993 ± 0.199	1.988 ± 0.194	1.991 ± 0.201	3.616 ± 0.497
6−7	2.323 ± 0.718	3.214 ± 0.883	1.983 ± 0.197	1.997 ± 0.188	2.001 ± 0.216	3.854 ± 0.709
7−8	3.997 ± 1.482	2.257 ± 0.573	1.996 ± 0.211	2.033 ± 0.267	2.261 ± 0.573	3.804 ± 0.763

[a]HBond1: O5-H16, HBond2:O3-H16, HBond3:O1-H1, HBond4: H46-O2, HBond5: H61-O8, HBond6: H61-O8 (see Scheme 1 for the labeling).

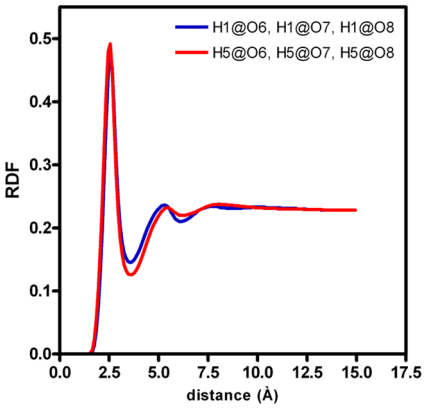

Figure 10. Radial distribution functions (RDFs) for the interactions of solvents donors (**H1** stands for the hydrogen in primary hydroxyl, and **H5** stands for the hydrogen in secondary hydroxyl) with the gelator acceptors.

Table 5. Calculated Maximum Loaded Npx (%w_d/w_g) by Gelators (6 mg) in Different Solvents

	N^2L/N^6Lys	N^2M/N^6Lys	N^2P/N^6Lys
LEE	33.3	166.6	116.6
1-decanol	100	125	166.6
1,2-propandiol	16.6	166.6	150
liquid paraffin	130	166.6	133.3

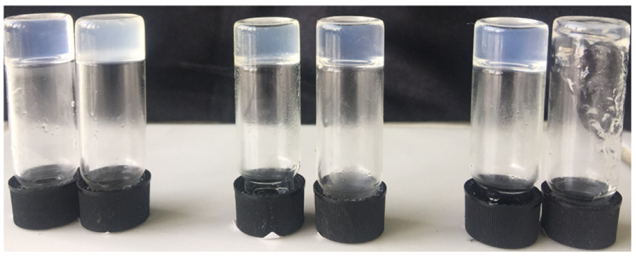

Figure 11. Comparision of images of unloaded (left) gels and gels loaded (right) with Npx (3.0 mg) composed of **N^2M/N^6Lys** (4.0 mg) from left in 1 mL of 1-decanol, MIE, and liquid paraffin.

confidence (r = >0.99).[66,67] Examples of the fitness of data to the Higuchi equation are shown in Figure 12. They all follow the Higuchi equation (eq 3) with good confidences.

3.4.2.1. Effect of Concentration of Npx. Since the drug cumulative release quantity was low from **N^2M/N^6Lys** (4.0 mg) gel in liquid paraffin (1.0 mL), the effect of Npx concentration on the cumulative release quantity was studied in this gel system at pH 7.4 (0.1 M phosphate buffer) and 25 °C. The results are presented in Figure 12 (see data in Table S10). They show that the cumulative release quantity increases with increasing loaded Npx, where at lower concentrations (0.5−1.5 mg), the difference is not large and at higher concentrations (3 and 5 mg), the gap in the release rate is parabolically enhanced (Figure 12). This is possibly due to the degradation of the gel structure in the presence of the larger loaded Npx. And also cumulative released amount of Npx increases with increasing quantity of loaded drug (Figure 13).

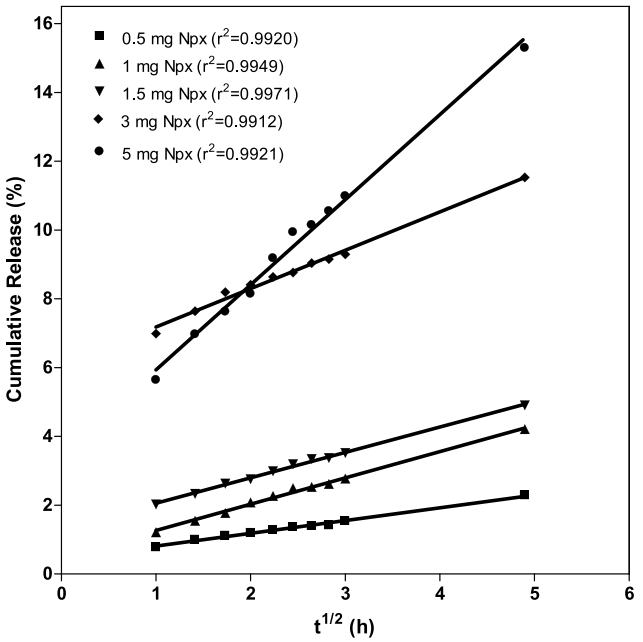

Figure 12. Time-dependent cumulative release of Npx from **N^2M/N^6Lys** gel prepared in liquid paraffin at pH 7.4 (0.1 M phosphate buffer) containing different concentrations of loaded Npx and 25 °C. Data are fitted to eq 3. The numbers are the mean values of three parallel experiments.

3.4.2.2. Effect of Solvent. **N^2P/N^6Lys** has a high drug loading capacity in all of the tested fluids. Hence, the effect of solvent on the drug release was investigated with **N^2P/N^6Lys** gelator. The gel forms of **N^2P/N^6Lys** (6 mg) containing Npx (3 mg) are prepared in 1 mL of four different solvents (LEE, 1-decanol, 1,2-propandiol, and liquid paraffin). The data regarding the release of Npx from these gels into 6 mL of the buffered solution (0.1 M phosphate) at pH 7.4 and 25 °C are shown in Figure 14 (see data in Table S8). The cumulative release is 10% after 24 h in liquid paraffin, while this is 40% in polar aprotic LEE, 27 and 30% in polar protic 1-decanol and 1,2-propanediol, respectively. They show that the release is favored in polar fluids, probably due to favorable interactions of polar gel liquids with water. So, this offers an opportunity for

DOI: 10.1021/acsomega.9b01086
ACS Omega 2019, 4, 12342−12356

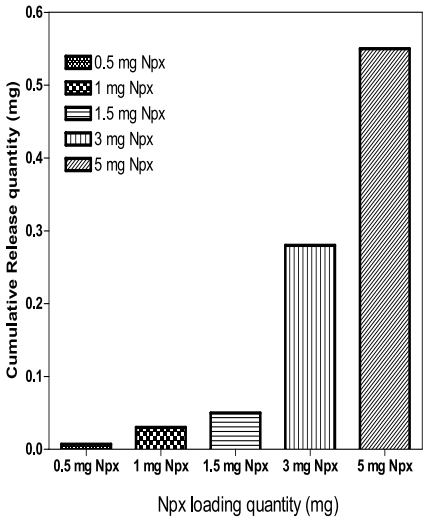

Figure 13. Cumulative release profiles from Npx-loaded **N^2M/N^6Lys** gel (4 mg gelator in 1 mL of liquid paraffin) in the presence of different loaded Npx concentrations at pH 7.4 (0.1 M phosphate buffer) and 25 °C for the first 9 h period. The numbers are the mean values of three parallel experiments.

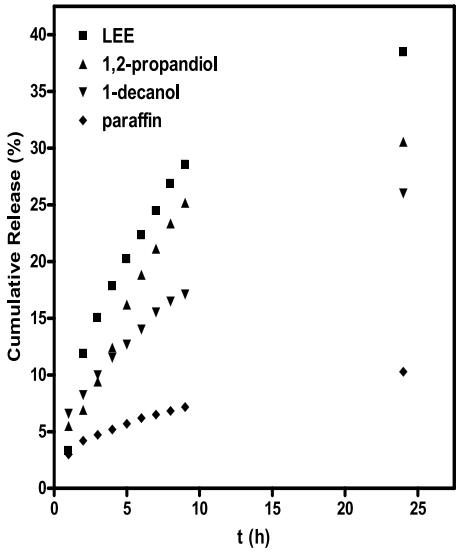

Figure 14. Time-dependent cumulative release as a percentage of Npx (3 mg) from **N^2P/N^6Lys** gel (6 mg gelator in 1 mL of different solvents) at pH 7.4 (0.1 M phosphate buffer) and at 25 °C. The numbers are the mean values of three parallel experiments.

controlling the time-dependent release rate of the drug (Figure 14).

3.4.2.3. Effect of pH. Topical delivery system has many advantages to bypass first-pass metabolism. pH changes play an essential role to avoid the risks and inconveniences of intravenous therapy and various absorption conditions.[68] The effect of pH on the release of Npx was studied in LEE since the highest release is observed (40% within 24 h) in this solvent, and therefore, it is expected that the measurement error will be minimized. The results are represented in Figure 15 (see data in Table S9). They demonstrate that the release showed dependence on pH, where it is slower at lower pH. This may be associated with the ionization degree of Npx. It would be fully ionized at higher pHs, and therefore, it would be expected to have an enhanced partition into water phase from the gel at

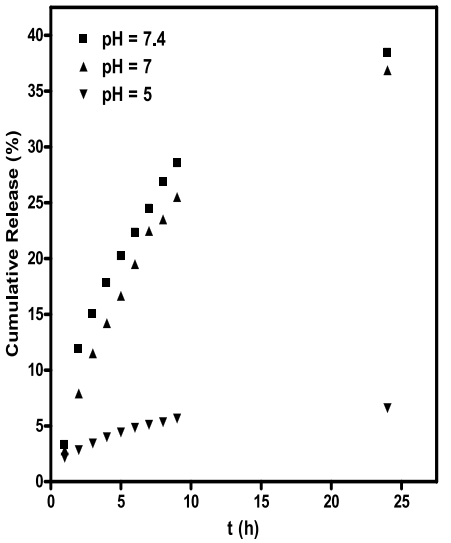

Figure 15. Effect of pH on the time-dependent cumulative release as a percentage of Npx from **N^2P/N^6Lys** gel prepared in LEE at 25 °C. The numbers are the mean values of three parallel experiments.

these pHs. In other words, at lower pH, the neutral form of the drug would predominate, and consequently, its partition rate into water phase would be declined since this form likely tends to interact with the gel network instead of water phase. The significance of the dependence of the release rate of Npx on pH may be recognized in the different routes of administration such as in skin,[69] ophthalmic,[70] and vagina.[71,72]

3.4.2.4. Effect of Gelator Concentration. The changes in the release rate of Npx with time from the gelators (**N^2L/N^6Lys**, **N^2M/N^6Lys**, and **N^2P/N^6Lys**) prepared in paraffin at two different concentrations (4.0 and 6.0 mg) are shown in Figure 16 (see data in Table S11). They indicated, as expected, that the increase in the concentration of the gelators reduces

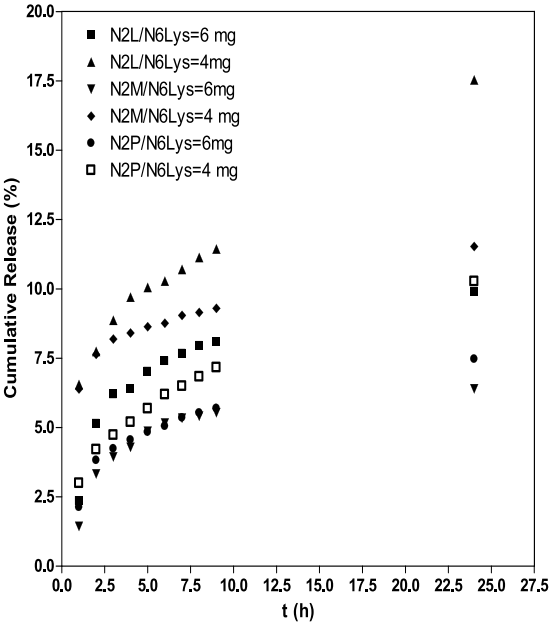

Figure 16. Time-dependent cumulative release of Npx (3 mg) from liquid paraffin gel containing different concentrations of gelators at pH 7.4 (0.1 M phosphate buffer) and 25 °C. The numbers are the mean values of three parallel experiments.

DOI: 10.1021/acsomega.9b01086
ACS Omega 2019, 4, 12342−12356

the release rate of Npx from the gels. Increasing gelator concentration may lead to the formation of more complicated gel matrix and hence possibly causes a decrease in the releasing of Npx from this matrix. Diffusion-controlled drug release is supplied by the solid skeletal network formed by the gelator molecules. The gelator aggregates or fibers, which are responsible for the three-dimensional structural network, immobilize the liquid via cross-linking and therefore the higher amounts of the gelator would acts as an obstacle to the passage of the drug out of the matrix. Thus, this could be employed as a beneficial way in adjusting the drug release rate. The difference in the release rate from the gels is likely associated with the strength of the gel matrices in the presence of the drug. So, the higher rate means the weaker interaction of Npx and hence the less stable gel matrix. So, it appears that **N^2L/N^6Lys** forms less stable gel than **N^2M/N^6Lys** and **N^2P/N^6Lys** in the presence of Npx (Figure 16).

4. CONCLUSIONS

This study represents the preparation of three new low-molecular-weight organogelators from constructed natural materials and their gelation behaviors in cosmetic solvents. Rheological measurements and in vitro drug release studies provided data that these gels could be promising candidates as drug delivery matrix. Data also indicated that these systems have a wide range of opportunities to control the release rate and route of administration, which could be controlled by adjusting some parameters such as solvent, concentration of gelator, pH, and length of alkanoyl. Computational calculations offer very useful approach for the prediction of structural and molecular dynamic properties of gel systems. However, higher level of theories is needed to have a better understanding of these complex systems.

■ ASSOCIATED CONTENT

Supporting Information

The Supporting Information is available free of charge on the ACS Publications website at DOI: 10.1021/acsomega.9b01086.

^{1}H, ^{13}C NMR, and IR spectra of all of the compounds and their GC−MS data; effect of gelator concentration on gel−sol transition temperature in the solvents studied; van't Hoff plots for the gels prepared in the solvents studied; time-dependent release rate of Npx from the gels in the solvent studied at pH 7.4 (0.1 M phosphate buffer) and 25 °C; 3D structure of octamer in mol2 format obtained from AM1 calculation; and 3D structure of octamer in 1,2-propandiol obtained from MD simulations (PDF)

■ AUTHOR INFORMATION

Corresponding Author

*E-mail. pirincn@dicle.edu.tr. Phone. +90 (0412) 2488550 (ext. 3055). Fax. +90 (0412) 2488300.

ORCID

Necmettin Pirinccioglu: 0000-0001-9805-9745

Notes

The authors declare no competing financial interest.

■ ACKNOWLEDGMENTS

The authors thank The Scientific and Technological Research Council of Turkey (TUBITAK) for financially supporting this research (Project No. 113Z142). They extend their thanks to the Dicle University, Research and Project Council, for supporting their project (No. 13-FF-72). They acknowledge DA Case (University of California, San Francisco) for a waiver license for AMBER (v.9 and v.11). They thank Professor Adnan Hayaloğlu (Inönü University, Malatya) for rheometrical measurements.

■ REFERENCES

(1) Das, D.; Kar, T.; Das, P. K. Gel-nanocomposites: materials with promising applications. *Soft Matter.* **2012**, *8*, 2348−2365.

(2) Díaz, D. D.; Kühbeck, D.; Koopmans, R. J. Stimuli-responsive gels as reaction vessels and reusable catalysts. *Chem. Soc. Rev.* **2011**, *40*, 427−448.

(3) Xu, B. Gels as Functional Nanomaterials for Biology and Medicine. *Langmuir* **2009**, *25*, 8375−8377.

(4) Ye, E.; Chee, P. L.; Prasad, A.; Fang, X.; Owh, C.; Yeo, V. J. J.; Loh, X. J. Supramolecular soft biomaterials for biomedical applications. *Mater. Today* **2014**, *17*, 194−202.

(5) Chai, Q.; Jiao, Y.; Yu, X. Hydrogels for Biomedical Applications: Their Characteristics and the Mechanisms behind Them. *Gels* **2017**, *3*, 6−21.

(6) Ohsedo, Y. Low-Molecular-Weight Gelators as Base Materials for Ointments. *Gels* **2016**, *2*, 13−24.

(7) Tian, R.; Chen, J.; Niu, R. The development of low-molecular weight hydrogels for applications in cancer therapy. *Nanoscale* **2014**, *6*, 3474−3482.

(8) Peppas, N. A.; Bures, P.; Leobandung, W.; Ichikawa, H. Hydrogels in pharmaceutical formulations. *Eur. J. Pharm. Biopharm.* **2000**, *50*, 27−46.

(9) Webber, M. J.; Appel, E. A.; Meijer, E. W.; Langer, R. Supramolecular biomaterials. *Nat. Mater.* **2016**, *15*, 13−26.

(10) Sage, L. V.; Lakshminarayanan, V.; Mendes, E.; Eelkema, R.; Esch, J. V. Dynamic supramolecular hydrogelators A biomedical perspective. *Chem. Today* **2014**, *32*, 62−66.

(11) Vicario-de-la-Torre, M.; Forcada, J. The Potential of Stimuli-Responsive Nanogels in Drug and Active Molecule Delivery for Targeted Therapy. *Gels* **2017**, *3*, 16−53.

(12) Hubbell, J. A.; Chilkoti, A. Nanomaterials for drug delivery. *Science* **2012**, *337*, 303−305.

(13) Schmidt-Mende, L.; MacManus-Driscoll, J. L. ZnO − nanostructures, defects, and devices. *Mater. Today* **2007**, *10*, 40−48.

(14) Zhang, L.; Wang, X.; Wang, T.; Liu, M. Tuning Soft Nanostructures in Self-assembled Supramolecular Gels: From Morphology Control to Morphology-Dependent Functions. *Small* **2015**, *11*, 1025−1038.

(15) Tomasini, C.; Castellucci, N. Peptides and peptidomimetics that behave as low molecular weight gelators. *Chem. Soc. Rev.* **2013**, *42*, 156−172.

(16) Mayr, J.; Saldías, C.; Díaz, D. D. Release of small bioactive molecules from physical gels. *Chem. Soc. Rev.* **2018**, *47*, 1484−1515.

(17) Menger, F. M.; Caran, K. L. Anatomy of a Gel. Amino Acid Derivatives That Rigidify Water at Submillimolar Concentrations. *J. Am. Chem. Soc.* **2000**, *122*, 11679−11691.

(18) Hanabusa, K.; Hiroko, N.; Mutsumi, K.; Hirofusa, S. Easy Preparation and Prominent Gelation of New Gelator Based on L-Lysine. *Chem. Lett.* **2000**, *29*, 1070−1071.

(19) Willemen, H. M.; Vermonden, T.; Marcelis, A. T. M.; Sudhölter, E. J. R. N-Cholyl amino acid alkyl esters−a novel class of organogelators. *Eur. J. Org. Chem.* **2001**, 2329−2335.

(20) Luo, X.; Lin, B.; Liang, Y. Self-assembled organogels formed by mono-chain L-alanine derivatives. *Chem. Commun.* **2001**, 1556−1557.

(21) Dasgupta, A.; Mitra, R. N.; Roy, S.; Das, P. K. Asymmetric resolution in ester reduction by $NaBH_4$ at the interface of aqueous

DOI: 10.1021/acsomega.9b01086
ACS Omega 2019, 4, 12342−12356

aggregates of amino acid, peptide, and chiral-counterion-based cationic surfactants. *Chem. Asian J.* **2006**, *1*, 780−788.
(22) Makarević, J.; Kokić, M.; Perić, B.; Tomišić, V.; Prodić, B. K.; Zinić, M. Bis-Amino Acid. Oxalyl Amides as Ambidextrous Gelators of Water and Organic Solvents: Supramolecular Gels with Temperature Dependent Assembly/Dissolution Equilibrium. *Chem. − Eur. J.* **2001**, *7*, 3328−3341.
(23) Becerril, J.; Burguete, M. I.; Escuder, B.; Luis, S. V.; Miravet, J. F.; Querol, M. Minimalist peptidomimetic cyclophanes as strong organogelators. *Chem. Commun.* **2002**, *7*, 738−739.
(24) Jokić, M.; Makarevic, J.; Zinic, M. A novel type of small organic gelators: bis-amino acid. oxalyl amides. *J. Chem. Soc. Chem. Commun.* **1995**, *17*, 1723−1724.
(25) Stock, H. T.; Turner, N. J.; McCague, R. J. *N*-2-carboxybenzoyl.-L-phenylalanylglycine: a low molecular-mass gelling agent. *J. Chem. Soc. Chem. Commun.* **1995**, 2063−2064.
(26) Suzuki, M.; Sato, T.; Kurose, A.; Shirai, H.; Hanabusa, K. New low-molecular weight gelators based on L-valine and L-isoleucine with various terminal groups. *Tetrahedron Lett.* **2005**, *46*, 2741−2745.
(27) Suzuki, M.; Owa, S.; Kimura, M.; Kurose, A.; Shirai, H.; Hanabusa, K. Supramolecular hydrogels and organogels based on novel L-valine and L-isoleucine amphiphiles. *Tetrahedron Lett.* **2005**, *46*, 303−306.
(28) Roy, S.; Das, D.; Dasgupta, A.; Mitra, R. N.; Das, P. K. Amino Acid Based Cationic Surfactants in Aqueous Solution: Physicochemical Study and Application of Supramolecular Chirality in Ketone Reduction. *Langmuir* **2005**, *21*, 10398−10404.
(29) Roy, S.; Das, P. K. Antibacterial hydrogels of amino acid-based cationic amphiphiles. *Biotechnol. Bioeng.* **2008**, *100*, 756−764.
(30) Liu, X.; Fei, J.; Wang, A.; Cui, W.; Zhu, P.; Li, J. Transformation of Dipeptide-Based Organogels into Chiral Crystals by Cryogenic Treatment. *Angew. Chem., Int. Ed.* **2017**, *56*, 2660−2663.
(31) Li, X.; Fei, J.; Xu, Y.; Li, D.; Yuan, T.; Li, G.; Wang, C.; Li, J. A Photoinduced Reversible Phase Transition in a Dipeptide Supramolecular Assembly. *Angew. Chem., Int. Ed.* **2018**, *57*, 1903−1907.
(32) Gronwald, O.; Shinkai, S. Sugar-Integrated Gelators of Organic Solvents. *Chem.−Eur. J.* **2001**, *7*, 4328−4334.
(33) Friggeri, A.; Gronwald, O.; van Bommel, K. J. C.; Shinkai, S.; Reinhoudt, D. N. Charge-Transfer Phenomena in Novel, Dual-Component, Sugar-Based Organogels. *J. Am. Chem. Soc.* **2002**, *124*, 10754−10758.
(34) Kiyonaka, S.; Shinkai, S.; Hamachi, I. Combinatorial Library of Low Molecular-Weight Organo- and Hydrogelators Based on Glycosylated Amino Acid Derivatives by Solid-Phase Synthesis. *Chem. − Eur. J.* **2003**, *9*, 976−983.
(35) Peng, J.; Xia, H.; Liu, K.; Gao, D.; Yang, M.; Yan, N.; Fang, Y. Water-in-oil gel emulsions from a cholesterol derivative: Structure and unusual properties. *J. Colloid Interface Sci.* **2009**, *336*, 780−785.
(36) Suzuki, M.; Nigawara, T.; Yumoto, M.; Kimura, M.; Shirai, H.; Hanabusa, K. L-Lysine based gemini organogelators: their organogelation properties and thermally stable organogels. *Org. Biomol. Chem.* **2003**, *1*, 4124−4131.
(37) Uzan, S.; Barıs, D.; Colak, M.; Aydın, H.; Hosgoren, H. Organogels as novel carriers for dermal and topical drug delivery vehicles. *Tetrahedron* **2016**, *72*, 7517−7525.
(38) White, B. D.; Mallen, J.; Arnold, K. A.; Fronczek, F. R.; Gandour, R. D.; Gehrig, L. M. B.; Gokel, G. W. Peptide side-arm derivatives of lariat ethers and bibracchial lariat ethers: syntheses, cation binding properties, and solid state structural data. *J. Org. Chem.* **1989**, *54*, 937−947.
(39) Sanna, V.; Mariani, A.; Caria, G.; Sechi, M. Synthesis and evaluation of different fatty acid esters formulated into Precirol ATO-based lipid nanoparticles as vehicles for topical delivery. *Chem. Pharm. Bull.* **2009**, *57*, 680−684.
(40) Barış, D.; Şeker, S.; Hoşgören, H.; Toğrul, M. Synthesis of rigid and C-2-symmetric 18-crown-6 type macrocycles bearing diamide-diester groups: enantiomeric recognition for alpha-(1-naphthyl) ethylammonium perchlorate salts. *Tetrahedron: Asymmetry* **2010**, *21*, 1893−1899.
(41) Gronwald, O.; Shinkai, S. Sugar-integrated gelators of organic solvents. *Chem. − Eur. J.* **2001**, *7*, 4328−4334.
(42) Xudong, Y.; Li, Y.; Yin, Y.; Yu, D. A simple and colorimetric fluoride receptor and its fluoride-responsive organogel. *Mater. Sci. Eng. C.* **2012**, *32*, 1695−1698.
(43) Suzuki, M.; Saito, H.; Hanabusa, K. Two-component organogelators based on two L-amino acids: Effect of combination of L-amino acids on organogelation behavior. *Langmuir* **2009**, *25*, 8579−8585.
(44) Suzuki, M.; Yumoto, M.; Shirai, H.; Hanabusa, K. Supramolecular gels formed by amphiphilic low-molecular-weight gelators of N-alpha,N-epsilon-diacyl-L-lysine derivatives. *Chem. − Eur. J.* **2008**, *14*, 2133−2144.
(45) Seo, S. H.; Chang, J. Y. Organogels from 1H-Imidazole Amphiphiles: Entrapment of a Hydrophilic Drug into Strands of the Self-Assembled Amphiphiles. *Chem. Mater.* **2005**, *17*, 3249−3254.
(46) Zoebisch, E. G.; Healy, E. F.; et al. AM1: A New General Purpose Quantum Mechanical Molecular Model. *J. Am. Chem. Soc.* **1985**, *107*, 3902−3909.
(47) Frisch, M. J.; Trucks, G. W.; Schlegel, H. B.; Scuseria, G. E.; Robb, M. A.; Cheeseman, J. R.; Montgomery, J. A., Jr.; Vreven, T.; Kudin, K. N.; Burant, J. C.; Millam, J. M.; Iyengar, S. S.; Tomasi, J.; Barone, V.; Mennucci, B.; Cossi, M.; Scalmani, G.; Rega, N.; Petersson, G. A.; Nakatsuji, H.; Hada, M.; Ehara, M.; Toyota, K.; Fukuda, R.; Hasegawa, J.; Ishida, M.; Nakajima, T.; Honda, Y.; Kitao, O.; Nakai, H.; Klene, M.; Li, X.; Knox, J. E.; Hratchian, H. P.; Cross, J. B.; Bakken, V.; Adamo, C.; Jaramillo, J.; Gomperts, R.; Stratmann, R. E.; Yazyev, O.; Austin, A. J.; Cammi, R.; Pomelli, C.; Ochterski, J. W.; Ayala, P. Y.; Morokuma, K.; Voth, G. A.; Salvador, P.; Dannenberg, J. J.; Zakrzewski, V. G.; Dapprich, S.; Daniels, A. D.; Strain, M. C.; Farkas, O.; Malick, D. K.; Rabuck, A. D.; Raghavachari, K.; Foresman, J. B.; Ortiz, J. V.; Cui, Q.; Baboul, A. G.; Clifford, S.; Cioslowski, J.; Stefanov, B. B.; Liu, G.; Liashenko, A.; Piskorz, P.; Komaromi, I.; Martin, R. L.; Fox, D. J.; Keith, T.; Al-Laham, M. A.; Peng, C. Y.; Nanayakkara, A.; Challacombe, M.; Gill, P. M. W.; Johnson, B.; Chen, W.; Wong, M. W.; Gonzalez, C.; Pople, J. A. *Gaussian 03*, revision C.02; Gaussian, Inc.: Wallingford, CT, 2004.
(48) Case, D. A.; Darden, T. A.; Cheatham, T. E., III.; Simmerling, C. L.; Wang, J.; Duke, R. E.; Luo, R.; Walker, R. C.; Zhang, W.; Merz, K. M.; Roberts, B.; Wang, B.; Hayik, S.; Roitberg, A.; Seabra, G.; Kolossváry, I.; Wong, K. F.; Paesani, F.; Vanicek, J.; Liu, J.; Wu, X.; Brozell, S. R.; Steinbrecher, T.; Gohlke, H.; Cai, Q.; Ye, X.; Wang, J.; Hsieh, M-J.; Cui, G.; Roe, D. R.; Mathews, D. H.; Seetin, M. G.; Sagui, C.; Babin, V.; Luchko, T.; Gusarov, S.; Kovalenko, A.; Kollman, P. A. *AMBER 11*; University of California: San Francisco, 2010.
(49) Jakalian, A.; Jack, D. B.; Bayly, C. I. Fast, efficient generation of high-quality atomic charges AM1-BCC model: II Parameterization and validation. *J. Comput. Chem.* **2002**, *23*, 1623−1641.
(50) Lee, M. C.; Duan, Y. Distinguish protein decoys by using a scoring function based on a new AMBER force field, short molecular dynamics simulations, and the generalized born solvent model. *Proteins* **2004**, *55*, 620−634.
(51) Wang, J. M.; Wolf, R. M.; Caldwell, J. W.; Kollman, P. A.; Case, D. A. Development and testing of a general amber force field. *J. Comput. Chem.* **2004**, *25*, 1157−1174.
(52) Accelrys Software Inc. A, Discovery Studio Modeling Environment, release 4.0, San Diego: Accelrys Software Inc. 2013.
(53) Cornell, W. D.; Cieplak, P.; Bayly, C. I.; Gould, I. R.; Merz, K. M.; Ferguson, D. M.; Spellneyer, D. C.; Fox, T.; Caldwell, J. W.; Kollman, P. A. A second generation force-field for the simulation of proteins, nucleic acids, and organic molecules. *J. Am. Chem. Soc.* **1995**, *117*, 5179−5197.
(54) Darden, T.; York, D.; Pedersen, L. Method for Ewald sums in large systems. *J. Chem Phys.* **1993**, *98*, 10089−10092.
(55) Pettersen, E. F.; Goddard, T. D.; Huang, C. C.; Couch, G. S.; Greenblatt, D. M.; Meng, E. C.; Ferin, T. E. UCSF Chimera-a

DOI: 10.1021/acsomega.9b01086
ACS Omega 2019, 4, 12342−12356

visualization system for exploratory research and analysis. *J. Comput. Chem.* **2004**, *25*, 1605−1612.
(56) Gao, C. Y.; Nicholson, D. M.; Keffer, D. J.; Edwards, B. J. A multiscale modeling demonstration based on the pair correlation function. *J. Non-Newtonian Fluid Mech.* **2008**, *152*, 140−147.
(57) Higuchi, T. Mechanism of sustained-action medication. Theoretical analysis of rate of release of solid drugs dispersed in solid matrices. *J. Pharm. Sci.* **1963**, *52*, 1145−1149.
(58) Suzuki, M.; Hanabusa, K. L-Lysine-based low-molecular-weight gelators. *Chem. Soc. Rev.* **2009**, *38*, 967−975.
(59) George, M.; Weiss, R. G. Molecular Organogels. Soft Matter Comprised of Low-Molecular-Mass Organic Gelators and Organic Liquids. *Acc. Chem. Res.* **2006**, *39*, 489−497.
(60) Pénzes, T.; Csóka, I.; Erös, I. Rheological analysis of the structural properties effecting the percutaneous absorption and stability in pharmaceutical organogels. *Rheol. Acta* **2004**, *43*, 457−463.
(61) Schramm, G. Some Theoretical Aspects of Dynamic Testing. *A Practical Approach to Rheology and Rheometry*; Schramm, G., Ed.; Gebrueder HAAKE GmbH: Karlsruhe, 1994.
(62) Brummer, R. *Rheology Essentials of Cosmetic and Food Emulsions*; Springer: Berlin, 2006.
(63) Baddi, S.; Madugula, S. S.; Sarma, D. S.; Yarasi Soujanya, Y.; Palanisamy, A. Combined Experimental and Computational Study of the Gelation of Cyclohexane-Based Bis(acyl-semicarbazides) and the Multi-Stimuli-Responsive Properties of Their Gels. *Langmuir* **2016**, *32*, 889−899.
(64) Celis, S.; Nolis, P.; Illa, O.; Branchadell, V.; Ortuño, R. M. Low-molecular-weight gelators consisting of hybrid cyclobutane-based peptides. *Org. Biomol. Chem.* **2013**, *11*, 2839−2846.
(65) Shikata, T.; Nishida, T.; Isare, B.; Linares, M.; Lazzaroni, R.; Bouteiller, L. Structure and Dynamics of a Bisurea-Based Supramolecular Polymer in n-Dodecane. *J. Phys. Chem. B* **2008**, *112*, 8459−8465.
(66) Peppas, N. A.; Narasimhan, B. Mathematical modeling in drug delivery: how modeling has shaped the way we design new drug delivery systems. *J. Controlled Release* **2014**, *190*, 75−81.
(67) Bruschi, M. L. *Strategies to Modify the Drug Release from Pharmaceutical Systems*; Woodhead Publishing, 2015.
(68) Verma, A.; Sukhdev, S.; Kaur, R.; Jain, U. K. Topical Gels as Drug Delivery Systems: A Review. *Int. J. Pharm. Sci. Rev. Res.* **2013**, *23*, 374−382.
(69) Rehman, K.; Zulfakar, M. H. Recent advances in gel technologies for topical and transdermal drug delivery. *Drug Dev. Ind. Pharm.* **2014**, *40*, 433−440.
(70) Kotreka, U. K.; Davis, V. L.; Adeyeye, M. C. Development of topical ophthalmic *In Situ* gel-forming estradiol delivery system intended for the prevention of age-related cataracts. *PLoS One* **2017**, 1−19.
(71) Johnson, T. A.; Greer, I. A.; Kelly, R. W.; Calder, A. A. The effect of pH on release of PGE2 from vaginal and endocervical preparations for induction of labour: an in-vitro study. *BJOG* **1992**, *99*, 877−880.
(72) Hussain, A.; Ahsa, F. The vagina as a route for systemic drug delivery. *J. Controlled Release* **2005**, *103*, 301−313.

DOI: 10.1021/acsomega.9b01086
ACS Omega 2019, 4, 12342−12356